

Supporting Information

Ethanol and KOH co-pretreatment towards ultra-high specific surface area carbons for high-rate and high-energy supercapacitors

2. Materials and Methods

2.1 Materials

Ethanol (99.9%), EMIMBF₄ (99 wt. %), and hydrochloric acid (36.0-38.0 wt. %), were purchased from Sigma-Aldrich Co. LLC. Pitaya peels were obtained from fruits supermarket. Potassium hydroxide (KOH, 99.9 wt. %) and Sodium sulphate (99.9 wt. %) were got from Macklin Inc. All the agents were analytical pure and used as received without further purification. The water used in the experiments was deionized (Milipore Mili-Q grade) with resistivity of 18.0 MΩ•cm.

2.2 Characterization

X-ray diffraction (XRD) patterns was collected by a X-ray diffraction (DX-2700, $\lambda = 1.5406 \text{ \AA}$). For the BET measurement, a Micromeritics Tristar 3020 instrument was used to evaluate the specific surface areas of the obtained carbons. All samples were dried at 80 °C in a vacuum oven for 12 h, following by degassing at 150 °C for 12 h. The morphology and structure of the products were observed on scanning electron microscope (SEM, Sigma 500/VP, the accelerate voltage was 5 kV) and transmission electron microscope (TEM, JEM-100SX, the accelerate voltage was 200 kV). X-ray photoelectron spectroscopic (XPS) measurements were carried out using X-ray photoelectron spectrometer (ESCALAB 250Xi, Thermo, USA). Raman and flourier transform infrared (FT-IR) spectra were obtained from Raman microspectrometer (Dilor LABRAM-1B) with an excitation wavelength of 532 nm and NEXUS-870 FTIR spectrometer (KBr pellet technique), respectively.

2.3 Materials synthesis

The pitaya peels were carefully washed with DI water to remove impurities and then annealed in a tube furnace at 400 °C in N₂ atmosphere for 2 h to obtain the carbon precursors. Afterwards the carbon precursors were mixed with KOH as the mass ratio of 1:2, 1:3, and 1:4 by adding 80 ml of different solutions (water, 60 vol. %, 70 vol. %, and 80 vol. % ethanol aqueous solution) in 100 ml beakers, respectively. Then the as-prepared blends were sonicated for 30 min to form the uniform suspensions. After that, all blends were heated to 100 °C in an oven over night to procure dry pre-treated carbon precursors. Subsequently, the pre-treated carbon precursors were activated in the tube furnace at 400 °C for 1.5 h and further calcinated at 850, 900, and 950 °C respectively under N₂ maintaining for 2 h. After cooling down to room temperature naturally, the activated carbons were washed with DI water to pH 7.0 firstly and neutralized by 1 M HCl solution, further washing with DI water to pH 7.0. The final products were obtained after drying in an oven at 80 °C for hole night, which were named as WPPC and EPPC-1 to 7 individually (The details could be found in Table S1).

2.4 Electrochemical measurements

The electrochemical energy storage properties of the samples were measured in a three-electrode system with 6 M KOH electrolyte solution on CHI-660E, embracing Galvanostatic charge-discharge (GCD), cyclic voltammetry (CV), and electrochemical impedance spectroscopy (EIS). The active materials, acetylene black and polyvinylidene fluoride (PVDF) in a weight ratio of 8:1:1 were prepared as work electrode into N-Methyl pyrrolidone (NMP). After that, the slurry was painted onto nickel foam and dry at 80 °C for 12 h. The mass loading of each electrode was ca. 1 mg•cm⁻². Ag/AgCl electrode and Pt foil (1×1 cm) were employed as reference electrode and counter electrode, particularly. The specific capacitances of samples were calculated by GCD patterns according to the formulation as follow:

$$C_g = \frac{I \times \Delta t}{m \times \Delta U_{(1)}}$$

where C_g (F•g⁻¹), I (A), Δt (s), m (g), and ΔU (V) refer to specific capacitance, constant current, discharge time, the mass of active materials, and discharge potential excluding the IR drop, respectively.

The two-electrode symmetric supercapacitor (SC) devices were assembled to CR 2016 coin-type cell by using 6 M KOH, 1 M Na₂SO₄, and EMIMBF₄ as electrolytes individually at ambient temperature in a glove box. GCD and CV curves were conducted by using a CHI660E electrochemical workstation at room temperature.

The electrochemical capacitance was calculated using eqn (2):

$$C_s = 4C_{\text{cell}} = \frac{4 \times I \times \Delta t}{m \times \Delta V} \quad (2)$$

where C_s (F•g⁻¹) represents the specific capacitance of single electrode, C_{cell} (F•g⁻¹) represents the device capacitance, I (A), Δt (s), and ΔV (V) have the same definition as in eqn (1), and m (g) is the total mass of the active materials in the two electrodes.

The energy density (E , W h•kg⁻¹) and power density (P , W•kg⁻¹) of all devices were conducted by eqn (3) and eqn (4):

$$E = \frac{1}{7.2} C_{\text{cell}} \Delta V^2 \quad (3)$$

$$P = \frac{E \times 3600}{\Delta t} \quad (4)$$

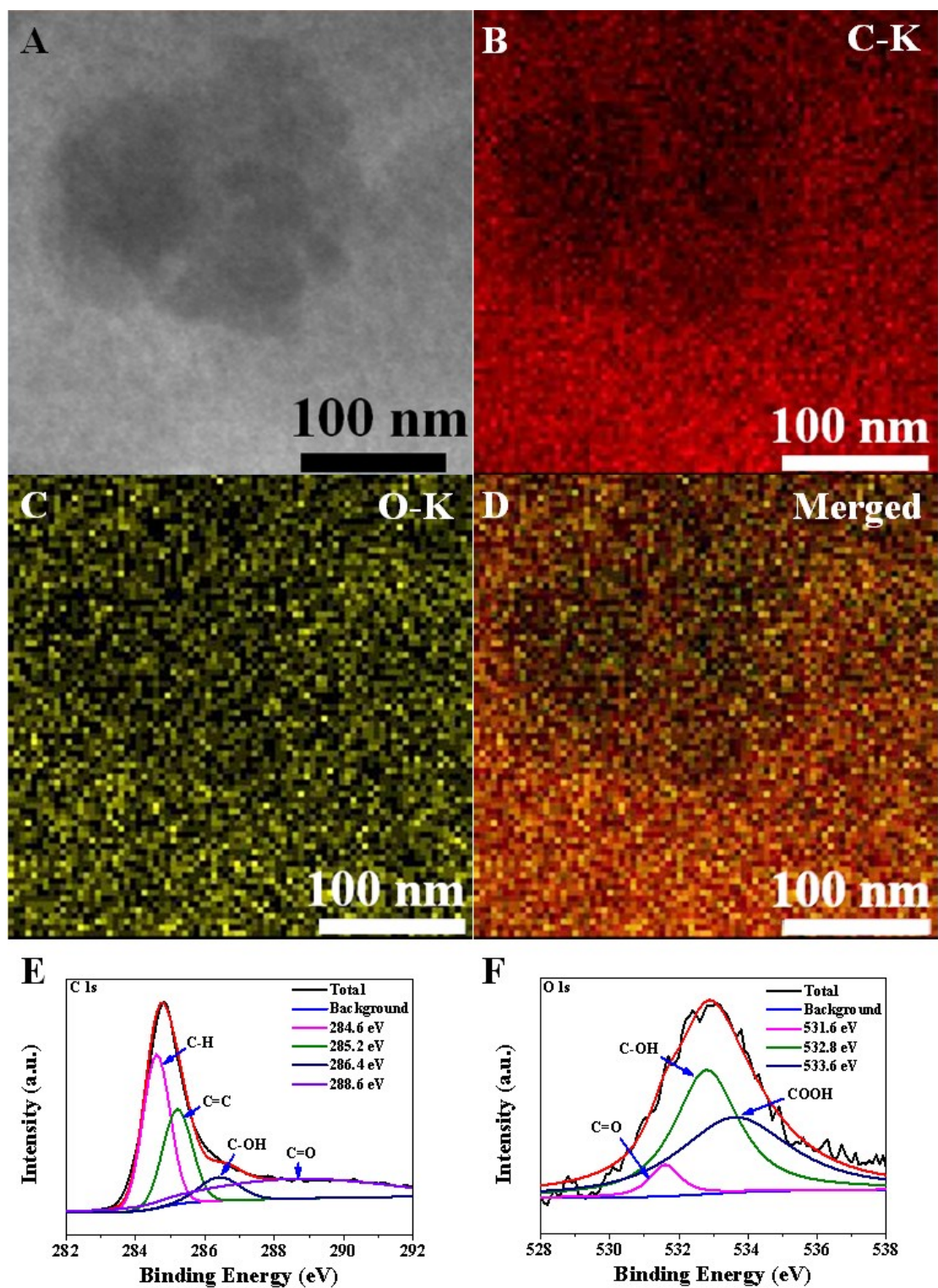


Figure S1. (A) TEM image of EPPC-2; Elemental mappings of (B) C, (C) O, and (D) the merged image; High-resolution spectra of (E) C 1s and (F) O 1s, respectively.

Table S1. List of abbreviations.

Full Spelling	Abbreviation
specific surface area	SSA
supercapacitors	SCs
lithium ion batteries	LIBs
symmetric supercapacitors	SSCs
carbons with water pretreatment	WPPC
carbons with ethanol pretreatment	EPPC
symmetric supercapacitors with KOH as electrolyte	EPPC-2 SSC-1
symmetric supercapacitors with Na ₂ SO ₄ as electrolyte	EPPC-2 SSC-2
symmetric supercapacitors with EMIMBF ₄ as electrolyte	EPPC-2 SSC-3

Table S2. Different pre-treatment conditions, mass ratios of carbon to KOH, and calcination temperatures for the influence of BET surface areas of the obtained carbons.

Sample	S_{BET} (m ² g ⁻¹)	Pre-treatment	Mass ratio of carbon to KOH	Calcination temperature (°C)
WPPC	1674.8	DI Water	1:3	900
EPPC-1	3396.8	60% Ethanol solution	1:3	900
EPPC-2	3521.4	70% Ethanol solution	1:3	900
EPPC-3	3269.3	80% Ethanol solution	1:3	900
EPPC-4	3429.2	70% Ethanol solution	1:3	850
EPPC-5	3472.6	70% Ethanol solution	1:3	950

EPPC-6	3126.2	70% Ethanol solution	1:2	900
EPPC-7	3202.5	70% Ethanol solution	1:4	900

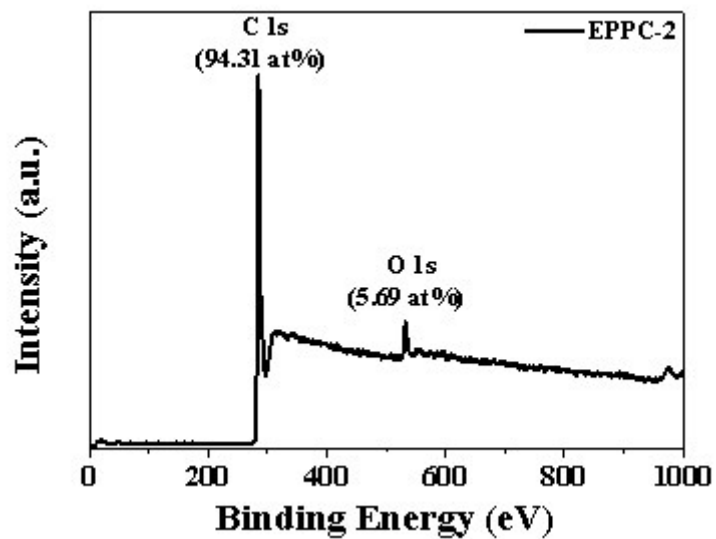


Figure S2. XPS survey profile of the EPPC-2.'

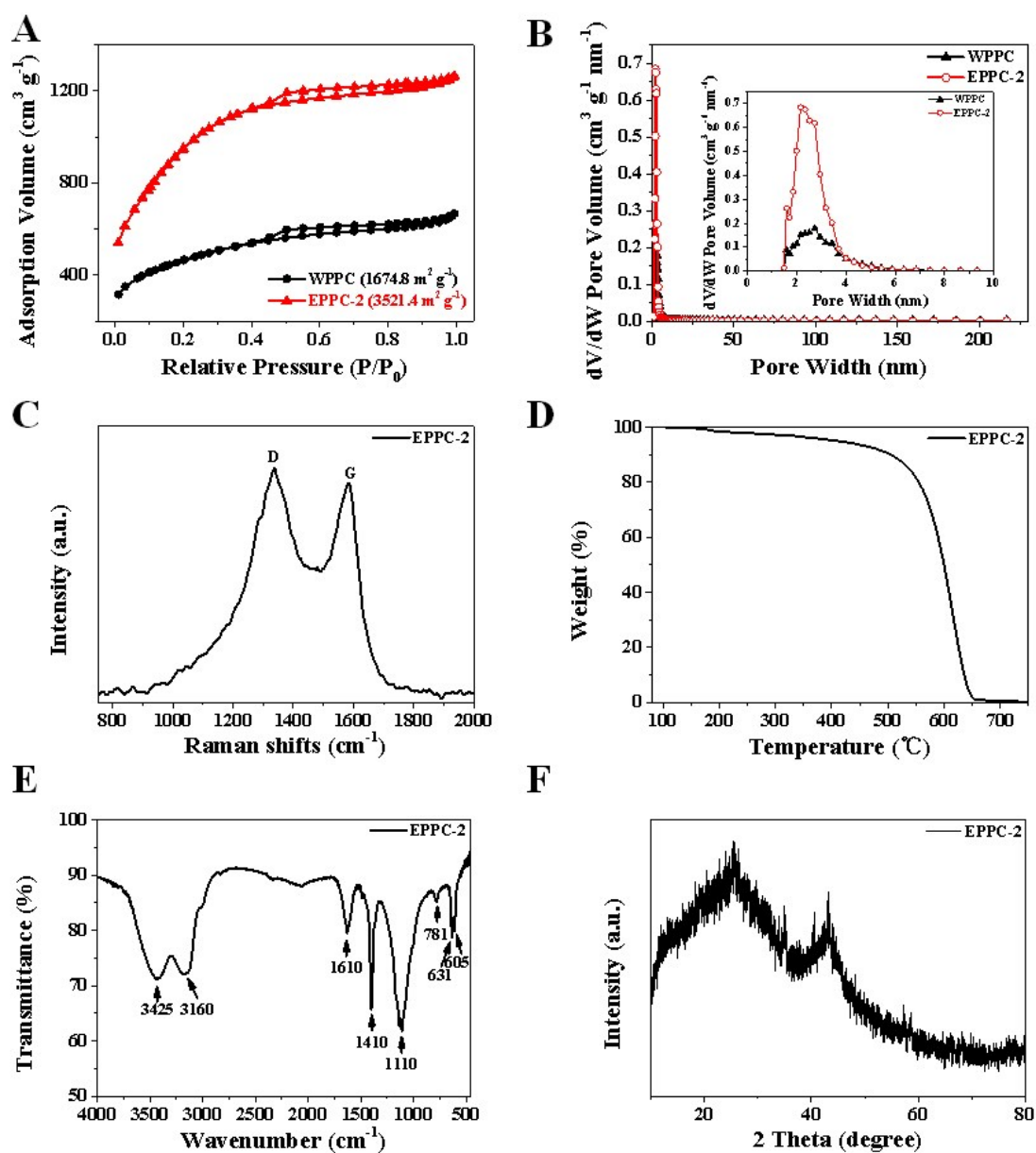


Figure S3. (A) N_2 sorption isotherms, and (B) pore size distribution curves for WPPC and EPPC-2; (C) Raman spectra, and (D) XRD pattern of WPPC and EPPC-2; (E) FTIR spectrum, and (F) Thermogravimetric curve under air condition of EPPC-2 respectively. The insert in (B) is the enlarged size distribution of WPPC and EPPC-2 ranging from 0-10 nm.

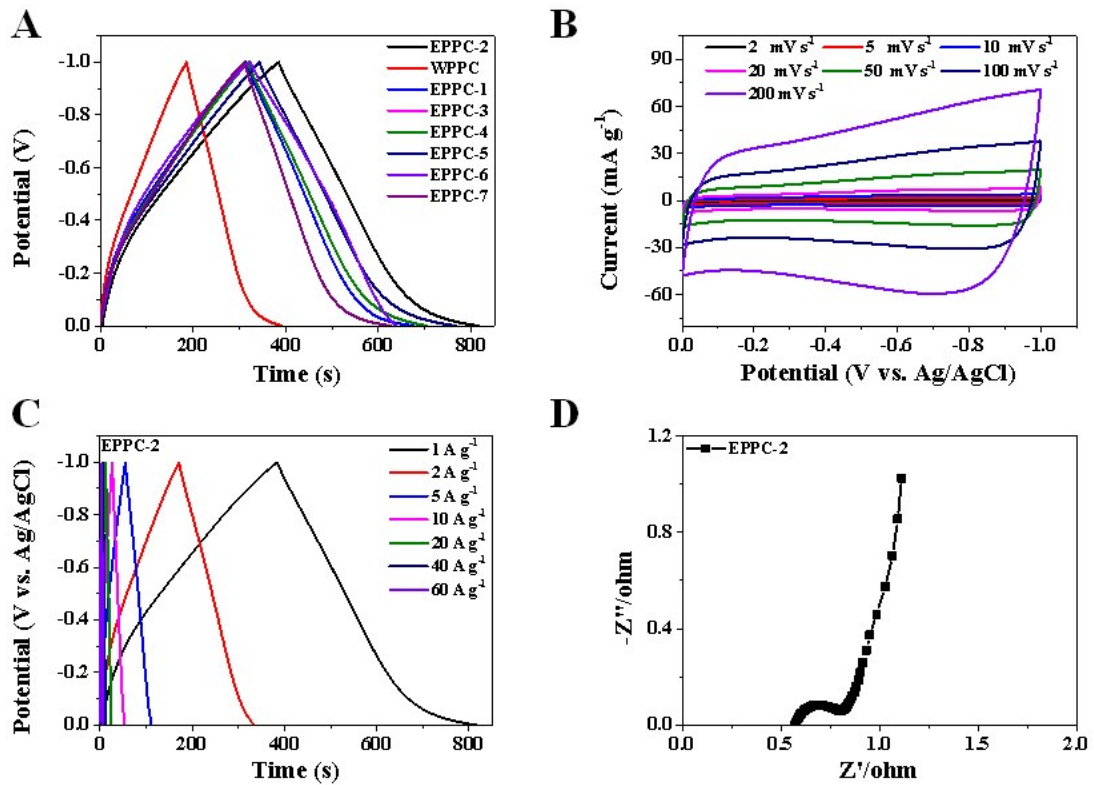


Figure S4. Electrochemical performance characteristics measured in a three-electrode system in the 6 M KOH electrolyte: (A) GCD curves of all samples at a current density of $1 \text{ A} \cdot \text{g}^{-1}$; (B) CV curves of EPPC-2 at different scan rates; (C) GCD curves of the EPPC-2 at different current densities; and (D) Nyquist plots of EPPC-2 as the negative electrode.

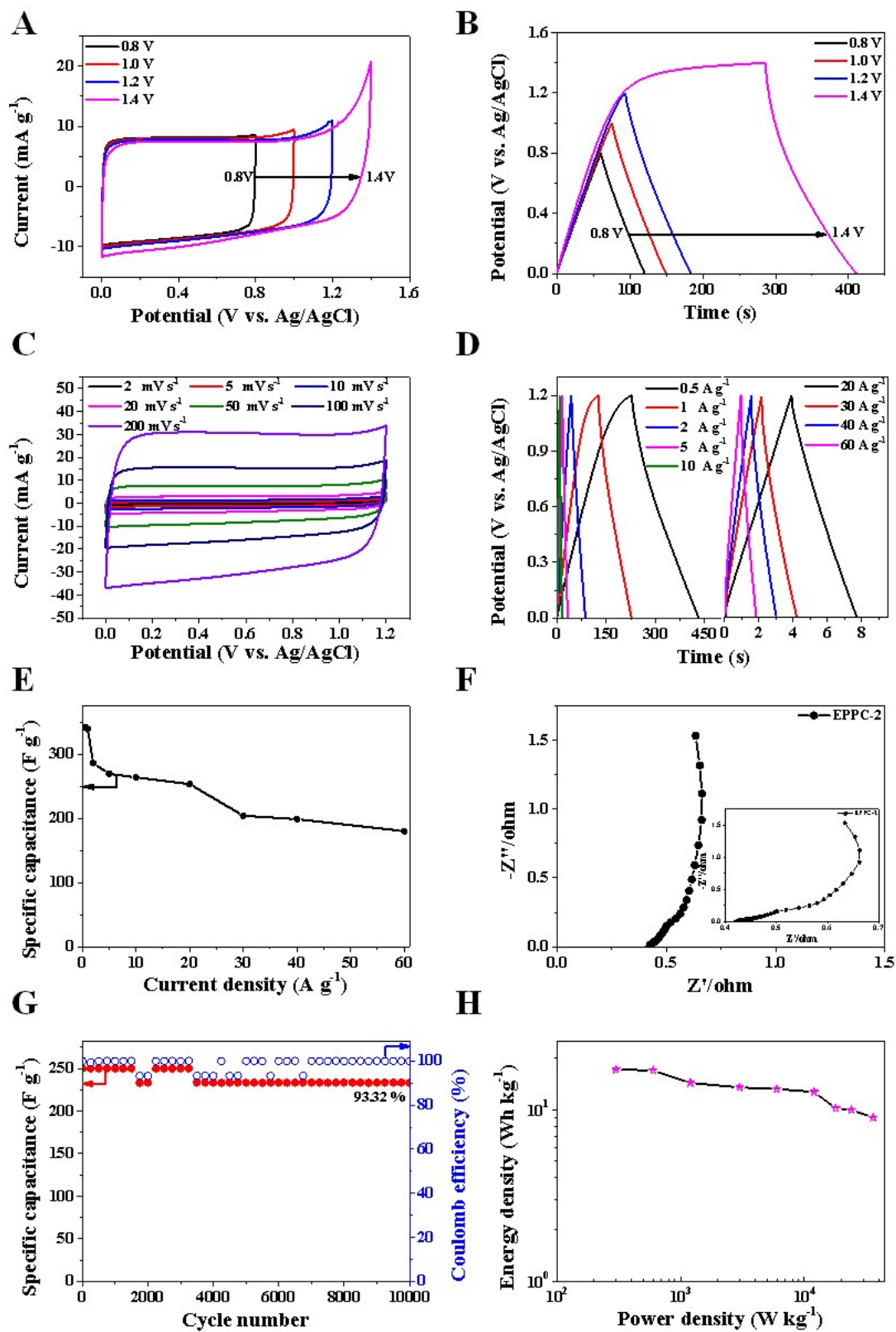


Figure S5. Electrochemical performance characteristics measured in a two-electrode SC in the 6 M KOH electrolyte (SSC-1): (A) CV curves of the SSC-1 operated in different voltage windows at a scan rate of $50 \text{ mV} \cdot \text{s}^{-1}$; (B) GCD curves of the SSC-1 operated in different voltage windows at $1 \text{ A} \cdot \text{g}^{-1}$; (C) CV

curves of the SSC-1 operated at different scan rates; (D) GCD curves of the SSC-1 operated at different current densities; (E) Specific capacitances for a single electrode at different current densities; (F) Nyquist plots of the SSC-1; (G) Cycling stability and Coulomb efficiency of the SSC-1 operated at the current density of $10 \text{ A} \cdot \text{g}^{-1}$; and (H) Ragone plot of the SSC-1

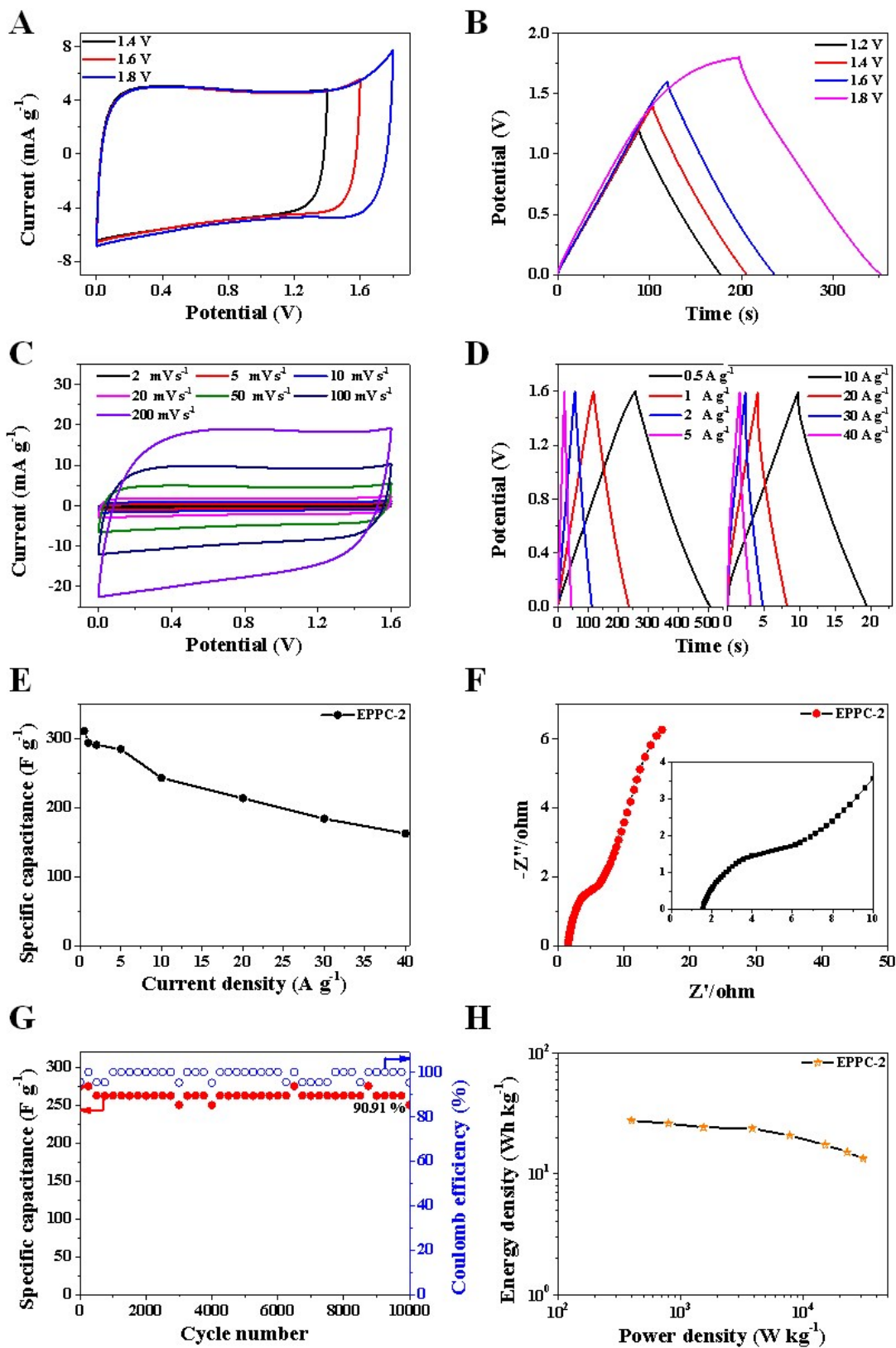


Figure S6. Electrochemical performance characteristics measured in a two-electrode SSC in the 1 M Na₂SO₄ electrolyte (SSC-2): (A) CV curves of the SSC-2 operated in different voltage windows at a scan rate of 50 mV·s⁻¹; (B) GCD curves of the SSC-2 operated in different voltage windows at 1 A·g⁻¹; (C) CV curves of the SSC-2 operated at different scan rates; (D) GCD curves of the SSC-2 operated at different current densities; (E) Specific capacitances for a single electrode at different current densities; (F) Nyquist plots of the SSC-2; (G) Cycling stability and Coulomb efficiency of the SSC-2 operated at the current density of 5 A·g⁻¹; and (H) Ragone plot of the SSC-2.

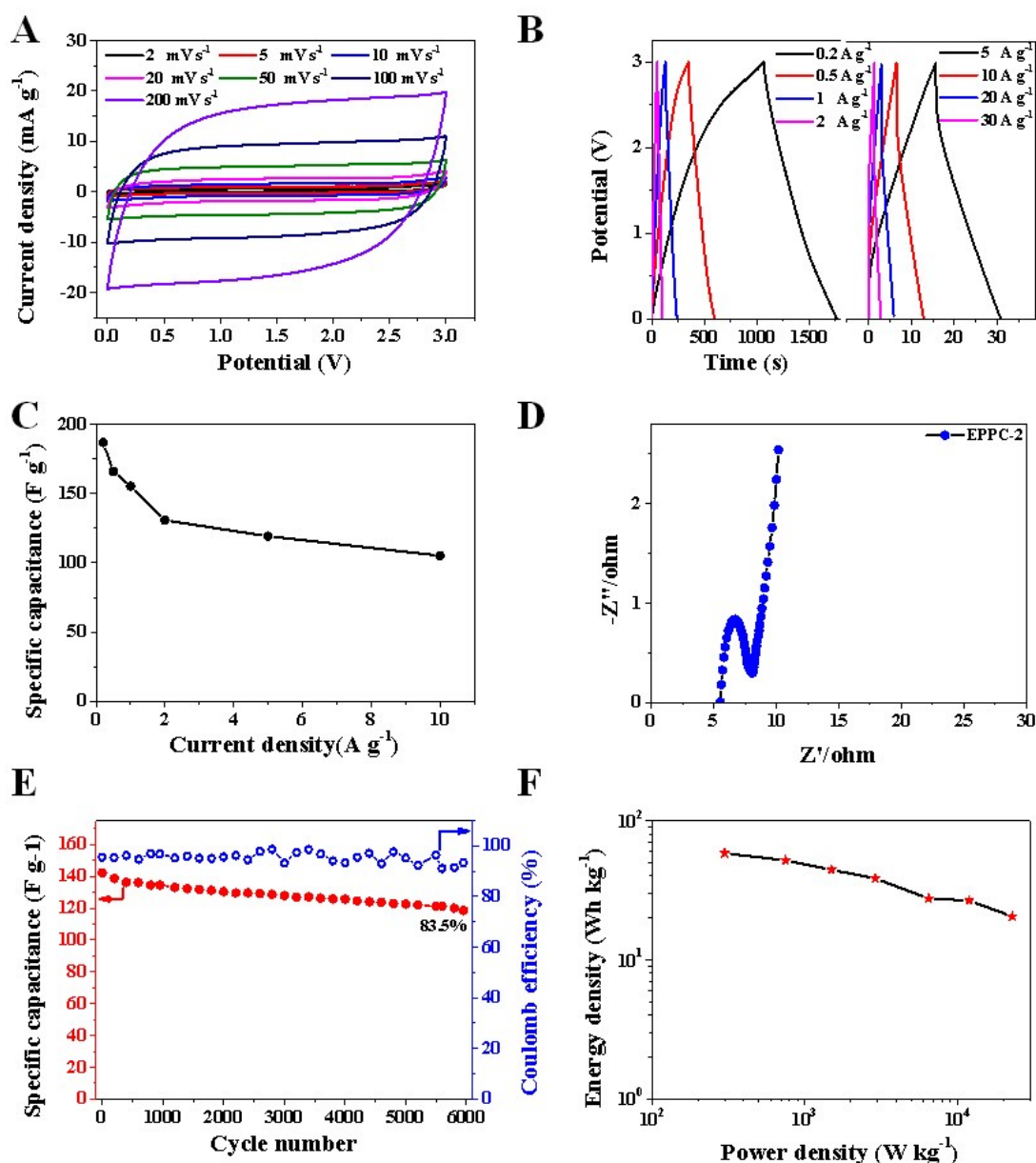


Figure S7. Electrochemical performance characteristics measured in a two-electrode SC in the EMIMBF₄ electrolyte (SSC-3): (A) CV curves of the SSC-3 operated at different scan rates; (B) GCD curves of the SSC-3 operated at different current densities; (C) Specific capacitances for a single electrode at different current densities; (D) Nyquist plots of the SSC-3; (E) Cycling stability and Coulomb efficiency

of the SSC-3 operated at the current density of 1 A·g⁻¹; and (F) Ragone plot of the SSC-3.

Table S3. Supercapacitor performances of reported biomass-derived AC materials using aqueous electrolytes.

Carbon source	S _{BET} (m ² ·g ⁻¹)	Test system/Electrolyte	Max Energy density (Wh·kg ⁻¹)	Power density (W·kg ⁻¹)	Ref.
Pitaya peel	3521.4	2/6M KOH 2/1 M Na ₂ SO ₄	17.1 27.6	300 400	This work
Bagasse	2296	2/1 M Na ₂ SO ₄	6.25	100.5	1
Cotton	1716	2/1 M H ₂ SO ₄	9.6	72	2
Melamine	1570	2/6 M KOH	9.2	23	3
Camellia petals	1122	2/6 M KOH	7.8	250	4
Ground cherry calyces	1612	2/6 M KOH	12.2	25	5
Rape pollen	2488	2/1 M Na ₂ SO ₄	26.8	181.4	6
Kraft lignin	1307	2/6 M KOH	8.5	100	7
Phenolic resins	1618	2/1 M Na ₂ SO ₄	16.97	200	8

Table S4. Supercapacitor performances of reported biomass-derived AC materials using ILs electrolytes.

Carbon source	S _{BET} (m ² ·g ⁻¹)	Electrolyte	Max Energy density (Wh·kg ⁻¹)	Power density (W·kg ⁻¹)	Ref.
Pitaya peel	3521.4	EMIMBF ₄	57.7	300	This work
Active carbon	-	EMIMBF ₄	30.13	874.8	9

Graphene	2406	EMIMBF ₄	55.7	55.9	10
Charcoals	3270	1 M TEABF ₄ /AN	42	390	11
Tobacco rods	1886	1M Et ₄ NBF ₄	31.3	500	12
Sunflower stalk	1505	Et ₄ NBF ₄	35.7	989	13
Tremella	1097	Et ₄ NBF ₄	42.4	760	14
Straw cellulose waste	2297	Et ₄ NBF ₄	28.6	14090	15
Sodium carboxymethyl cellulose	1275	EMIMBF ₄	42	4500	16

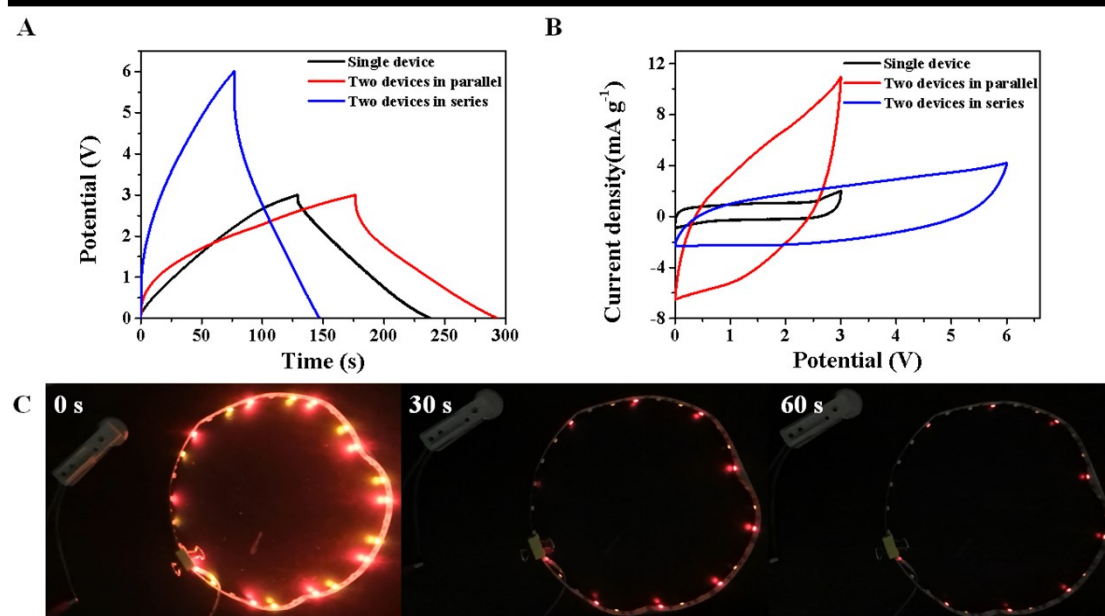


Figure S8. (A) GCD curves and (B) CV curves of two SSC-3 devices connected in series and in parallel, at a current density of 1 A·g⁻¹ and scan rate of 50 mV·s⁻¹. (C) Photographs of commercial colorful LED lights with different time powered by two SSC-3 devices in series.

References

1. H. Feng, H. Hu, H. Dong, Y. Xiao, Y. Cai, B. Lei, Y. Liu and M. Zheng, *J Power Sources*, 2016, **302**, 164-173.
2. H. Wang, H. Yi, C. Zhu, X. Wang and H. J. Fan, *Nano Energy*, 2015, **13**, 658-669.

3. F. Sun, J. Gao, X. Pi, L. Wang, Y. Yang, Z. Qu and S. Wu, *J Power Sources*, 2017, **337**, 189-196.
4. T. Wei, X. Wei, L. Yang, H. Xiao, Y. Gao and H. Li, *J Power Sources*, 2016, **331**, 373-381.
5. D. Yu, C. Chen, G. Zhao, L. Sun, B. Du, H. Zhang, Z. Li, Y. Sun, F. Besenbacher and M. Yu, *Chemsuschem*, 2018, **11**, 1678-1685.
6. S. Liu, Y. Liang, W. Zhou, W. Hu, H. Dong, M. Zheng, H. Hu, B. Lei, Y. Xiao and Y. Liu, *J Mater Chem A*, 2018, **6**, 12046-12055.
7. F. Liu, Z. Wang, H. Zhang, L. Jin, X. Chu, B. Gu, H. Huang and W. Yang, *Carbon*, 2019, **149**, 105-116.
8. J. Guo, D. Wu, T. Wang and Y. Ma, *Applied Surface Science*, 2019, **475**, 56-66.
9. X. Zhong, J. Tang, L. Cao, W. Kong, Z. Sun, H. Cheng, Z. Lu, H. Pan and B. Xu, *Electrochim Acta*, 2017, **244**, 112-118.
10. C. Zheng, X. Zhou, H. Cao, G. Wang and Z. Liu, *J Mater Chem A*, 2015, **3**, 9543-9549.
11. D. M. Kang, Q. L. Liu, J. J. Gu, Y. S. Su, W. Zhang and D. Zhang, *Acs Nano*, 2015, **9**, 11225-11233.
12. Y.-Q. Zhao, M. Lu, P.-Y. Tao, Y.-J. Zhang, X.-T. Gong, Z. Yang, G.-Q. Zhang and H.-L. Li, *J Power Sources*, 2016, **307**, 391-400.
13. X. Wang, S. Yun, W. Fang, C. Zhang, X. Liang, Z. Lei and Z. Liu, *ACS Sustainable Chemistry & Engineering*, 2018, **6**, 11397-11407.
14. D. Chen, L. Li, Y. Xi, J. Li, M. Lu, J. Cao and W. Han, *Electrochim Acta*, 2018, **286**, 264-270.
15. Z. Chen, X. Wang, B. Xue, Q. Wei, L. Hu, Z. Wang, X. Yang and J. Qiu, *Chemsuschem*, 2019, **12**, 1390-1400.
16. D. D. Chen, Z. Q. He, M. Wang, D. Wu, X. Y. Chen and Z. J. Zhang, *J Solid State Electr*, 2020, **24**, 641-654.